The role of magnetic resonance spectroscopy in differentiation of neoplastic from non-neoplastic pediatric intracerebral brain lesions

Ghada Mahmoud Korany[a], Samy A. El Aziz Sayed[b], Noha M. Ali[b], Khaled F. Ryad[c]

[a]Department of Diagnostic Radiology, [b]Department of Radiodiagnosis, Faculty of Medicine, Assiut University, Assiut, [c]Department of Pediatric Oncology, South Egypt Cancer Institute, Assiut, Egypt

Correspondence to Ghada Mahmoud Korany, MBBCH,
Department of Diagnostic Radiology, Assiut University, Assiut, Egypt
Tel: +20 101 316 0106;
Fax: 020862585484
e-mail: ghada. 202020@yahoo.com

Received 23 September 2019
Revised 13 October 2019
Accepted 15 October 2019
Published 09 October 2021

Journal of Current Medical Research and Practice
2021, 6:270–275

Background
Pediatric brain tumors are considered a significant health problem and present several imaging challenges. The role of imaging is no longer limited to merely providing anatomical details. In this research, we explained the role of magnetic resonance spectroscopy (MRS) in the differentiation of neoplastic from non-neoplastic intracerebral brain lesions in pediatric patients. The aim was to assess the role of MRS in pediatric brain tumors by discrimination between tumors and tumor-like lesions, differentiation between primary and secondary neoplasms, differentiation between high-grade and low-grade tumors, and determination of tumor extension.

Patients and methods
A total of 30 pediatric patients with cerebral lesions were examined by MRS. Choline (Cho), creatine (cr), *N*-acetylaspartate (NAA), and lipid-lactate peaks were evaluated. Of the 30 patients, 26 underwent stereotactic biopsy. Histopathological results were compared with the MRS results.

Results
Diagnostic accuracy of spectroscopic data for prediction of neoplastic lesions in the current study was assessed. Regarding Cho/NAA, a cutoff point greater than 2 had 88% sensitivity and 75% specificity for prediction of neoplastic lesions, with areas under the curve (AUC) of 0.91 ($P = 0.01$). Regarding Cho/Cr, a cutoff point greater than 1.86 had 85% sensitivity and 75% specificity for prediction of neoplastic lesions, with AUC of 0.85 ($P = 0.02$). Regarding Cho/NAA+Cr, a cutoff point greater than 0.8 had 88% sensitivity and 100% specificity for prediction of neoplastic lesions, with AUC of 0.91 ($P = 0.009$).

Conclusion
MRS can potentially overcome the limitations of sampling errors with histopathologic grading of the tumor for determining the most optimal therapy regimen and regularity and aggressiveness of postoperative follow-up and treatment.

Keywords:
brain neoplasms, magnetic resonance imaging, magnetic resonance spectroscopy, stereotactic biopsy

J Curr Med Res Pract 6:270–275

2357-0121

Introduction

Noninvasive and accurate differentiation between neoplastic and non-neoplastic brain lesions is important in determining the correct treatment and, in some cases, may avoid the necessity of performing a biopsy [1]. Conventional MRI provides important information regarding the contrast material enhancement, perienhancement edema, distant tumor foci, hemorrhage, necrosis, and mass effect, which are helpful in characterizing tumor aggressiveness. However, magnetic resonance spectroscopy (MRS) offers additional information related to tumor proliferation and metabolism or neuronal damage [2].

MRS is the use of magnetic resonance in the quantification of metabolites and the study of their distribution in different tissues. Rather than displaying MRI proton signals on a gray scale as an image depending on the relative signal strength, MRS displays the quantities as a spectrum [3].

There is a wide list of metabolites that may be useful in the MRS evaluation of brain tumors, including: *N*-acetylaspartate (NAA), choline (Cho), creatine (cr), lipids, lactate, alanine, and myoinositol [2].

Most studies published have used long echo times (TE) and have focused on evaluating

abnormalities of NAA, total choline (tCho), and lactate (Lac) by analysis of ratios relative to creatine (Cr) [4].

Short TE MRS permits the observation of more metabolites, and the spectra are superior with respect to signal intensity-to-noise ratio. At the same time, fully automated postprocessing software providing robust quantitative output has become available. Elevated taurine (τ), an amino acid that has not been detected with long TE MRS, has recently been observed independently in medulloblastoma by several groups using short TE MRS and was found to be an important differentiator of this tumor type from other common pediatric brain tumors [4].

Aim

This study aims to assess the role of MRS in pediatric brain tumors by discrimination between tumors and tumor-like lesions, differentiation between primary and secondary neoplasms, differentiation between high-grade and low-grade tumors, and determination of tumor extension.

Patients and methods

This study was performed at Radiodiagnosis Department, Assiut University Hospital. Thirty patients in the pediatric age group ranging between 1 and 17 years were subjected to thorough history taking and clinical examination, conventional MRI, and MRS study. The study was approved by the Local Ethics Committee of Faculty of Medicine, Assiut University. Written informed consent was obtained from participants' parents before enrolment.

Patient inclusion criterion was as follows:

(1) An intracerebral space occupying lesion/lesions detected on conventional structural imaging.

Patient exclusion criteria were as follows:

(1) Extensively hemorrhagic lesion.
(2) Fat-containing lesion or very adjacent to the scalp fat or skull base.

Methods

All patients were subjected to the following: detailed clinical data, including personal data, and different systemic and neurological complaints.

Detailed clinical examination included general and neurological examinations.

Conventional MRI

The examinations were carried out in the following sequence:

(1) Sedation for irritable patients.
(2) Instructions to minimize head motion.
(3) Removal of any prohibited materials before entering the magnet's room.
(4) Contrast material: Gad-DTPA (Magnevist or Omniscan), 0.1 mmol/kg.
(5) Receiver head coil.

Philips Achevia 1.5-T system was used for imaging (1.5 Tesla MRI system (Achieva; Philips Medical systems, Best, The Netherlands)), with following sequences:

Axial and sagittal T1-weighted spinecho.

Axial FLAIR.

Axial and coronal T2-weighted fast spinecho.

Then contrast-enhanced axial, sagittal, and coronal T1-weighted spinecho images.

Magnetic resonance spectroscopy

Maximum high Cho/NAA, Cho/Cr, and Cho/NAA+Cr at intermediate TE 144 ms and ml/Cr at short TE 35 ms peak ratios in the lesions are recorded.

Maximum low NAA/Cho and NAA/Cr at intermediate TE are recorded.

Cho/NAA and Cho/Cr at intermediate TE 144 ms at the perilesional edema, if present, are recorded.

Lipid signal presence or absence is recorded.

These are achieved using the following: first, 2D MRSI PRESS at intermediate TE 144 ms. Cubic voxels of either 2 or 1.5 cm length were used depending on the size of the tumor inside the spectroscopic grid and the spectroscopic grid is extended and manually adjusted to include lesion, edema if present, and normal brain tissue (5 min). Second, 2D short TE sequence at 35 ms. Cubic voxels of either 2 or 1.5 cm length were used depending on the size of the tumor inside the spectroscopic grid, and the spectroscopic grid is extended and manually adjusted to include lesion, edema, if present, and normal brain tissue (12 min).

The peak ratios can be obtained by measuring and comparing areas under the curve (AUC).

The peaks are assigned as follows: Cho peak at 3.2 ppm, Cr at 3 ppm, NAA peak at 2.02 ppm, mobile lipids at 0.5–1.5 ppm, lactate 1.44 ppm, and mI at 3.56 ppm.

Statistical analysis

It was done using SPSS version 18. Quantitative data were expressed in mean and SD, whereas qualitative data were expressed in frequency and percentages. The diagnostic performance of the used metabolite ratios was evaluated using receiver operating characteristic curve analysis.

Results

It included 30 patients and their age ranged between 1 and 17 years, with a mean ± SD of 11.56 ± 2.48 years. Of the studied patients, 16 (53.3%) patients were females with a mean ± SD of 9.63 ± 2.09 years, whereas 14 (41.7%) patients were males, with a mean ± SD of 13.9 ± 2.2 years.

Final diagnosis in the studied patients

The final diagnosis in the studied patients was obtained either by histopathological examination or by confirmation with clinical with laboratory diagnosis and follow-up.

(1) Histopathological diagnosis: the final diagnosis was obtained by histopathological evaluation in 26/30 (86.7%) patients as follows:
   (a) Primary high-grade neoplasms presented in 10 (33.3%%) patients [four (13.4%) cases with high grade astrocytoma, two (6.7%) cases with medulloblastoma, two (6.7%) cases with anaplastic ependymoma, one (3.3%) case with choroid plexus carcinoma, and one (3.3%) case with primitive neuroectodermal tumor] (Fig. 1).
   (b) Primary low-grade neoplasms presented in 12 (40%) patients [seven (23.3%) cases with low-grade astrocytoma, two (6.7%) cases with ependymoma, two (6.7%) case with pleomorphic xanthoastrocytoma, and one (3.3%) case with dysembryoplastic neuroepithelial tumor] (Fig. 2).
   (c) Brain abscess in two (6.7%) cases.
   (d) Metastatic lesion from rhabdomyosarcoma in one (3.3%) case.
   (e) Local tumor recurrence in one (3.3%) case, proved to be glioblastoma multiform.
(2) The final diagnosis was confirmed by clinical with laboratory diagnosis with follow-up imaging in 4/30 (13.3%):
   (a) Two (6.7%) case with a brainstem tumor.
   (b) One (3.3%) case with multiple sclerosis.
   (c) One (3.3%) case with acute disseminated encephalomyelitis.

Figure 1

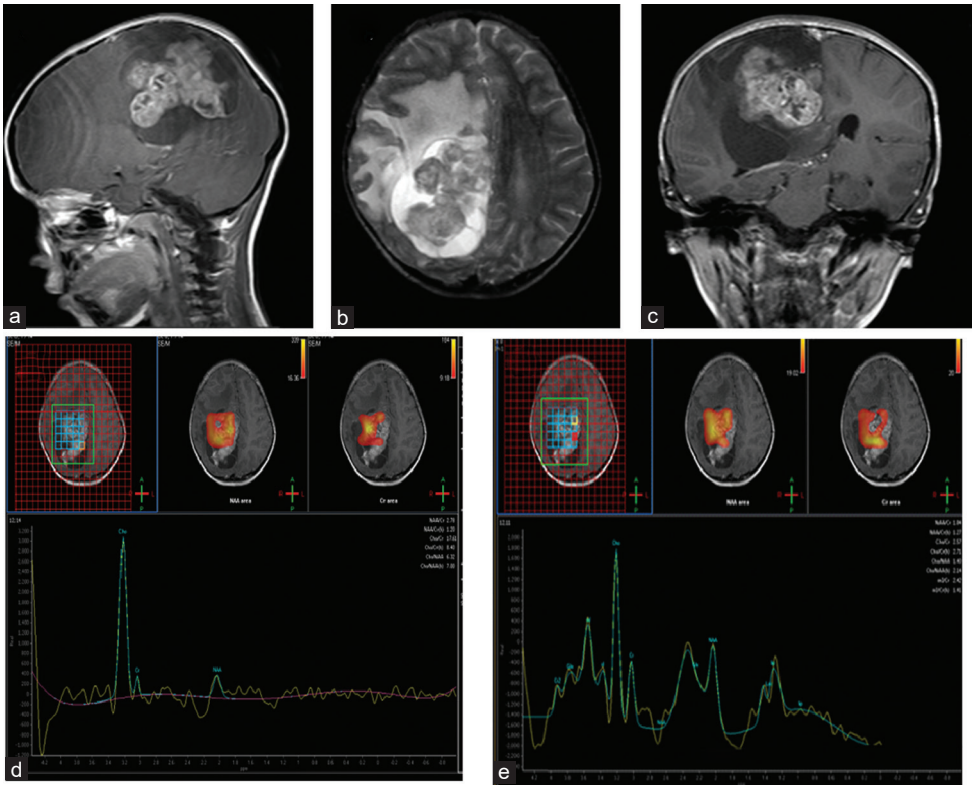

(a, b and c) Conventional imaging showing mass lesion seen implicating in the right parieto-occipital lobe. (d and e) 2D PRESS 144 ms echo spectrum shows remarkable elevation of choline peak with marked reduction of both *N*-acetylaspartate and creatine. Magnetic resonance spectroscopy diagnosis: primary high-grade glioma. With such distribution and ipsilateral ventricular dilatation, choroid plexus malignant featuring lesion is suggested. Histopathologically proven as choroid plexus carcinoma.

Figure 2

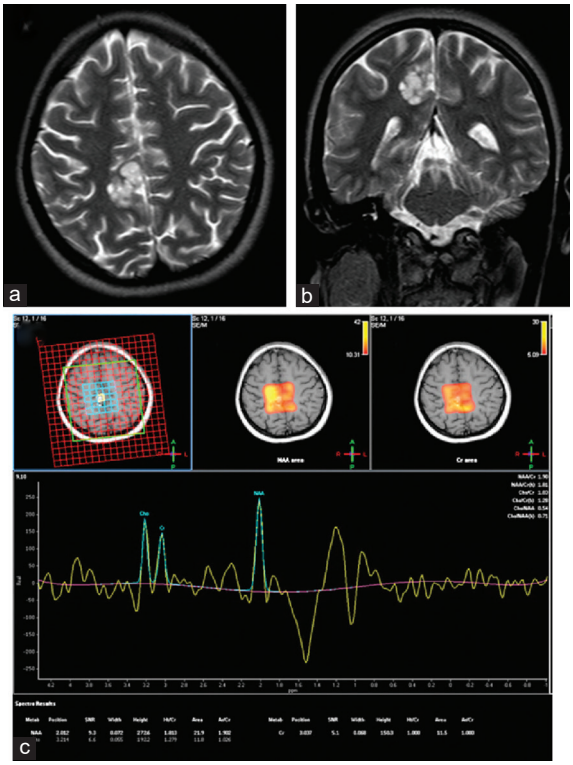

(a and b) Conventional imaging shows patchy enhancing lesion in the right high parietal lobe. (c) 2D PRESS 144 m/s echo spectrum in the lesion shows nearly normal metabolite spectrum apart from mild reduction of *N*-acetylaspartate and mild elevation of myoinositol peak (mI/Cr 1.3) and traces of lactate peak. Magnetic resonance spectroscopy diagnosis: primary low-grade glioma, but dysembryoplastic neuroepithelial tumor is highly suggested. Pathology revealed dysembryoplastic neuroepithelial tumor.

Based on the final diagnosis; 26 (86.7%) cases had neoplastic lesions while only four (13.3%) had non-neoplastic lesions (Table 1).

Magnetic resonance spectroscopic results

Diagnostic accuracy of spectroscopic data for prediction of neoplastic lesions in this study revealed the following (Tables 2 and 3):

(1) Regarding Cho/NAA, a cutoff point greater than 2 had 88% sensitivity and 75% specificity for prediction of neoplastic lesions, with AUC of 0.91 and $P = 0.01$.
(2) Regarding Cho/Cr, a cutoff point greater than 1.86 had 85% sensitivity and 75% specificity for prediction of neoplastic lesions, with AUC of 0.85 and $P = 0.02$.
(3) Regarding Cho/NAA + Cr, a cutoff point greater than 0.8 had 88% sensitivity and 100% specificity for prediction of neoplastic lesions, with AUC of 0.91 and $P = 0.009$.

Discussion

Conventional MRI provides only anatomic information, which radiologists interpret by means of visual inspection of signal intensities and geometric structures including mainly location of the lesion, contrast enhancement, edema, mass effect, necrosis, and hemorrhage [5].

Contrast enhancement only represents the disruption of the blood–brain barrier. Not all malignant tumors show contrast enhancement as one-third of nonenhancing tumors are in fact high-grade gliomas, whereas many low-grade tumors and non-neoplastic lesions show contrast enhancement [6].

Table 1 Distribution of final diagnosis among studied patients based on pathological diagnosis or clinical laboratory diagnosis and follow-up imaging

Method of final diagnosis	Nature	*n*=30
Histopathology		26 (86.7)
High-grade astrocytoma	Neoplastic lesion	4 (13.3)
Low-grade astrocytoma	Neoplastic lesion	7 (23.3)
Medulloblastoma	Neoplastic lesion	2 (6.7)
Ependymoma	Neoplastic lesion	2 (6.7)
Anaplastic ependymoma	Neoplastic lesion	2 (6.7)
PXA	Neoplastic lesion	2 (6.7)
Brain abscess	Non-neoplastic lesion	2 (6.7)
Choroid plexus carcinoma	Neoplastic lesion	1 (3.3)
Metastatic lesion	Neoplastic lesion	1 (3.3)
Recurrence of GBM	Neoplastic lesion	1 (3.3)
DNET	Neoplastic lesion	1 (3.3)
PNET	Neoplastic lesion	1 (3.3)
Clinical with laboratory diagnosis		4 (13.3)
Brainstem glioma	Neoplastic lesion	2 (6.7)
Multiple sclerosis	Non-neoplastic lesion	1 (3.3)
ADEM	Non-neoplastic lesion	1 (3.3)
Total		30

Data were expressed in the form of frequency (percentage). ADEM, acute disseminated encephalomyelitis; DENT, dysembryoplastic neuroepithelial tumor; PENT, primitive neuroectodermal tumor; PXA, pleomorphic xanthoastrocytoma.

Table 2 Spectroscopic data in the studied patients according to nature of lesions

	Neoplastic (*n*=26)	Non-neoplastic (*n*=4)	*P*
Cho/Cr	10.22±2.09	1.71±0.34	0.001
Cho/NAA	6.17±1.05	1.47±0.6	0.001
Cho/NAA+Cr	2.15±0.98	1.62±0.63	0.02
NAA/Cho	3.15±0.37	1.02±0.11	0.001
NAA/Cr	2.26±0.33	1.62±0.56	0.06

Data were expressed in form of mean and SD and compared with Mann–Whitney test. Cho, choline; Cr, creatine; NAA, *N*-acetylaspartate. $P<0.05$, significant.

Table 3 Diagnostic accuracy of spectroscopic data for prediction of neoplastic lesions in the current study

	Cho/NAA	Cho/Cr	Cho/NAA+Cr
Sensitivity (%)	88	85	88
Specificity (%)	75	75	100
Optimal cutoff	>2	>1.86	>0.8
AUC	0.91	0.85	0.91
P	0.01	0.02	0.009

AUC, area under the curve; Cho, choline; Cr, creatine; NAA, *N*-acetylaspartate. $P<0.05$, significant.

Conventional MRI is not able to depict changes in cell density, cell type, or biochemical composition. Lesions of different underlying pathophysiology can manifest with a similar MRI appearance, and even a single disease entity may have varied imaging findings, so anatomic imaging suffers from low specificity. Conventional imaging is also unable to accurately depict tumor infiltration outside the enhancing or T2 margin, which is crucial for preoperative decision making, intraoperative MRI-guided resections, and postoperative follow-up [7].

In advanced neuroimaging, MRS added physiologic data to the high spatial resolution of basic anatomic imaging obtained with conventional structural MRI. MRS provides information about biochemical characteristics, metabolic heterogeneity of the lesion, and surrounding brain tissue. DWI provides information about cellularity and structural integrity of the tissues [8].

Brain tumors are known for their metabolic heterogeneity, which is further aggravated by the presence of necrotic areas. Non-neoplastic lesions also show necrotic areas. So metabolite peak ratios will inevitably be heterogeneous; in necrotic areas, metabolite peak ratios are expected to be dwarfed whether neoplastic or non-neoplastic lesion [8].

In this study, regarding Cho/Cr, neoplastic lesions showed higher Cho/Cr ranging from 1.1 to 20, with mean ± SD of 10.22 ± 2.09; however, in non-neoplastic lesions, lower Cho/Cr ranging from 0.5 to 3.1 with mean ± SD of 1.71 ± 0.34. At a cutoff point greater than 1.86, it has 85% sensitivity and 75% specificity for prediction of neoplastic lesions, with AUC of 0.85 and $P = 0.02$.

This was in agreement with the study by Ozan and Ender [9] which reported that Cho/Cr greater than 1.98 shows sensitivity of 71.8% and specificity of 100% in the differentiation of neoplastic vs non-neoplastic lesions.

In this study, regarding Cho/NAA, neoplastic lesions showed higher Cho/NAA ranging from 0.6 to 11.5, with mean ± SD of 6.17 ± 1.05; however, non-neoplastic lesions showed lower Cho/NAA, ranging from 0.4 to 2.5, with mean ± SD of 1.47 ± 0.6. At a cutoff point greater than 2, it has 88% sensitivity and 75% specificity for prediction of neoplastic lesions, with AUC of 0.91 and $P = 0.01$.

This was in agreement with other studies such as Ozan and Ender [9], who reported that Cho/NAA greater than 1.83 shows sensitivity of 87.2 and specificity of 100%, and NAA/Cr less than or equal to 1.23 shows sensitivity of 84.6% and specificity of 57.1% in differentiation of neoplastic vs non-neoplastic lesions. Butzen *et al.* [3] reported that Cho/NAA greater than 1 shows sensitivity of 79% and specificity of 77% as an indicator of neoplastic process. McKnight *et al.* [10] reported that Cho/NAA ratio correlates with cell density and cell proliferation index; a ratio greater than 2 shows sensitivity of 96% and specificity of 70% in differentiating neoplastic vs non-neoplastic lesion.

In this study, regarding Cho/NAA+Cr, neoplastic lesions showed higher Cho/NAA+Cr, ranging from 0.4 to 5.4, with mean ± SD 2.15 ± 0.98; however, non-neoplastic lesions showed lower Cho/NAA + Cr, ranging from 0.2 to 3.2, with mean ± SD 1.62 ± 0.63 At a cutoff point greater than 0.8, it has 88% sensitivity and 100% specificity for prediction of neoplastic lesions, with AUC of 0.91 and $P = 0.009$.

Ozan and Ender [9] reported that Cho/NAA + Cr greater than 2.8 shows 84.6% sensitivity and 100% specificity in the differentiation of neoplastic vs non-neoplastic lesions.

Elevated Cho along with decreased NAA is typically regarded as a diagnostic feature of brain tumors [11].

With a normal NAA spectrum, a cerebral tumor becomes unlikely, yet very low grade or small lesions can show a normal NAA as well. In the latter, this is owing to the partial volume effect of adjacent healthy parenchyma [12].

From this study, we recommended the following:

(1) MRS should be used routinely as a valuable complementary noninvasive tool besides conventional MRI whenever available to reach a final diagnosis confidently.
(2) The use of multivoxel chemical shift imaging, by which spectra from numerous small voxels can be acquired, to enable great coverage of large tumors. It would also add the benefit of measuring the metabolite ratios in the edema, as peritumoral edema can be more valuable in detecting tumor grade.
(3) Combination of both short and intermediate TEs to achieve better sensitivity, specificity, and accuracy.

Limitation of the current study

MRS methods have limited brain coverage, limited to a few voxels or slices. Moreover, too small lesions are not amenable to study by MRS. In addition, some regions of the brain are unfavorable for MRS because of

magnetic susceptibility effects from nearby air spaces, or other artifacts. In these instances, MRS cannot be used.

Conclusion

Advanced MRI techniques, such as MRS, can give important in-vivo physiologic and metabolic information. Advanced neuroimaging had an important role in the differentiation of the neoplastic and non-neoplastic lesions and the grading of glioma. MRS can potentially overcome the limitations of sampling errors with histopathologic grading of tumor for determining the most optimal therapy regimen and regularity and aggressiveness of postoperative follow-up and treatment.

Financial support and sponsorship

Nil.

Conflicts of interest

There are no conflicts of interest.

References

1 Hourani R, Brant LJ, Rizk T, Weingart JD, Barker PB, Horská A. Can proton MR spectroscopic and perfusion imaging differentiate between neoplastic and nonneoplastic brain lesions in adults? Am J Neuroradiol 2008; 29:366–372.

2 Oz G, Alger JR, Barker PB, Bartha R, Bizzi A, Boesch C, *et al*. Clinical proton MR spectroscopy in central nervous system disorders. Radiology 2014; 270:658–679.

3 Butzen J, Prost R, Chetty V, Donahue K, Neppl R, Bowen W, *et al*. Discrimination between neoplastic and nonneoplastic brain lesions by use of proton MR spectroscopy: the limits of accuracy with a logistic regression model. Am J Neuroradiol 2000; 21:1213–1219.

4 JM García-Gómez, J Luts, M Julià-Sapé, P Krooshof, S Tortajada, JV Robledo, *et al*. Multiproject-multicenter evaluation of automatic brain tumor classification by magnetic resonance spectroscopy. Magn Reson Mater Phy 2009; 22:5–218.

5 Luthra G, Parihar A, Nath K, Jaiswal S, Prasad KN, Husain N, *et al*. Comparative evaluation of fungal, tubercular, and pyogenic brain abscesses with conventional and diffusion MR imaging and proton MR spectroscopy. Am J Neuroradiol 2006; 28:1332–1338.

6 Lev MH, Ozsunar Y, Henson JW, Rasheed AA, Barest GD, Harsh GR, *et al*. Glial tumor grading and outcome prediction using dynamic spin echo MR susceptibility mapping compared with conventional contrast enhanced MR. Am J Neuroradiol 2004; 25:214–221.

7 Young GS. Advanced MRI of adult brain tumors. Neurol Clin 2007; 25:947–973.

8 P Korfiatis, B Erickson. The basics of diffusion and perfusion imaging in brain tumors. Appl Radiol 2014; 423:156–167.

9 Karatağ O, Karatağ GY, Uysal E, Can SM, Ertürk M, Başak M, *et al*. Canmagnetic resonance spectroscopy adequately differentiate neoplastic from non-neoplastic and high grade from low grade lesions in brain masses? Marmara Med J 2010; 20:326–338.

10 McKnight TR, Lamborn KR, Love TD, Berger MS, Chang S, Dillon WP, *et al*. Correlation of magnetic resonance spectroscopic and growth characteristics within Grades II and III gliomas. J Neurosurg 2007; 106:660–666.

11 Howe FA, Barton SJ, Cudlip SA, Stubbs M, Saunders DE, Murphy M, *et al*. Metabolic profiles of human brain tumors using quantitative *in vivo* 1H magnetic resonance spectroscopy. Magn Reson Med 2003; 49:317–329.

12 Dowling C, Bollen AW, Noworolski SM, McDermott MW, Barbaro NM, Day MR, *et al*. Pre-operative proton MR spectroscopic imaging of brain tumors: correlation with histopathologic analysis of resection specimens. Am J Neuroradiol 2001; 22:604–612.